Published in final edited form as:
Behav Brain Res. 2014 July 15; 268: 127–138. doi:10.1016/j.bbr.2014.04.001.

A Large Scale (N = 102) Functional Neuroimaging Study of Error processing in a Go/NoGo Task

Vaughn R. Steele[a,b,e], **Eric D. Claus**[a], **Eyal Aharoni**[a,b], **Carla Harenski**[a], **Vince D. Calhoun**[a,b,c], **Godfrey Pearlson**[c,d], and **Kent A. Kiehl**[a,b]

[a]The nonprofit Mind Research Network (MRN) & Lovelace Biomedical and Environmental Research Institute (LBERI)

[b]University of New Mexico

[c]Yale University School of Medicine

[d]Olin Neuropsychiatry Research Center, Institute of Living

Abstract

We report a functional magnetic resonance imaging (fMRI) study of 102 healthy participants who completed a demanding Go/NoGo task. The primary purpose of this study was to delineate the neural systems underlying responses to errors in a large sample. We identified a number of regions engaged during error processing including the anterior cingulate, left lateral prefrontal areas and bilateral inferior frontal gyrus, and the subthalamic nucleus. The power afforded by the large cohort enabled identification of regions not consistently measured during Go/NoGo tasks thus helping to incrementally refine our understanding of the neural correlates of error processing. With the present fMRI results, in combination with our previous exploration of response inhibition (Steele et al. [1]), we outline a comprehensive set of regions associated with both response inhibition and error processing.

Keywords

error processing; fMRI; Go/NoGo; response inhibition

1. Introduction

A fuller understanding of the neural mechanisms that underlie error-monitoring and response inhibition would benefit several areas of cognitive neuroscience. Such information could facilitate greater understanding of these processes in both the theoretical and applied domains, particularly in understanding response inhibition and error-monitoring in

[e]Corresponding Author: The Mind Research Network, 1101 Yale Boulevard NE, Albuquerque, NM 87106. Phone: (505) 504-0182. Fax: (505) 272-8002. vsteele@unm.edu.

psychopathological samples. We previously published an analysis of response inhibition [1] in the same subject sample and present here companion analyses and thorough accounting of cognitive functions associated with response inhibition and error-monitoring with a large sample using functional magnetic resonance imaging (fMRI).

Response inhibition and error-monitoring (i.e., error processing) have been explored using several types of inhibition tasks (e.g., Go/NoGo, Stroop, Stop-signal, Flanker, Wisconsin Card Sorting Task, and Task-Switching: see [2] for review). We used a standard, previously published [3] Go/NoGo paradigm to measure response inhibition and error processing where participants are serially presented with targets (Go Stimuli), which require a response, and distractors(N oGo stimuli), which require inhibition of a response. In this task, as in other Go/NoGo tasks, the presentation of target stimuli is more frequent than distractors, creating a bias towards responding to target stimuli. Successful performance on this task requires the ability to monitor conflicts, process response errors, withhold or inhibit a pre-potent response, and learn from response errors. The task is well designed to distinguish the neuronal systems associated with response inhibition and error processing.

Neuroscience research has identified a number of brain areas related to successful response inhibition [1, 4]. This network includes the lateral and ventrolateral prefrontal cortex (e.g., [1, 5–8]), inferior frontal gyrus [1, 9–13], inferior parietal lobe (e.g., [1, 5, 10–12, 14, 15]), pre-supplementary motor areas [16] anterior cingulate cortex (ACC; e.g., [1, 3, 7, 10]), occipital regions such as the cuneus [1, 7, 17, 18] and subcortical regions including the thalamus and basal ganglia [1, 10, 14, 15, 19–21].

Neuroscience research has also identified brain areas responsible for error processing and, a few of these regions overlap with those observed in successful response inhibition [22–27]. One of the most comprehensive neurobiological models of error processing to date [28] postulates that the mesolimbic dopamine system sends input from the basal ganglia to the ACC (primarily rostral), which then evaluates response error patterns to be utilized in subsequent learning behavior. In addition to the ACC [3, 29–31] the amygdala [32] and dorsolateral prefrontal cortex [32, 33] have also been implicated in error processing. It is believed that the ACC relays error information from the frontal cortex and basal ganglia to motor areas. These motor areas modify behavioral plans by providing feedback to the frontal cortex and basal ganglia [34]. The dorsal portion of the ACC (dACC) has been most commonly associated with response conflict and perhaps error monitoring as well, while the rostral portion of the anterior cingulate (rACC) has been associated with the affective appraisal of error [3, 5, 17, 31, 35–37].

The primary focus of the current exploration is to thoroughly measure the networks involved in Go/NoGo tasks with a large sample. Although there is a growing body of evidence supporting the involvement of the regions discussed above from imaging and lesion studies [38–41] findings across studies are somewhat inconsistent. We have discussed this elsewhere [1] and only highlight these issues here. Variability in results of brain imaging studies could be due to a number of factors. One issue, small sample size, is known to hamper the ability to detect small effects (Type II error) in functional neuroimaging studies [42, 43]. This issue is also well addressed well in meta-analyses [2, 4, 11, 43]. Nevertheless,

early studies of cognitive control and inhibitory processing were largely comprised of relatively small sample sizes (i.e., n < 20) but more recent studies have employed more modest sample sizes or combined samples across studies [16, 32, 33, 44, 45]. Large sample sizes are necessary in functional neuroimaging studies to address inconsistencies in the literature and to develop a robust standard by which comparisons can be made to psychopathological groups.

We report here an fMRI investigation of 102 participants who completed a Go/NoGo task requiring the response inhibition of a pre-potent response [3]. We have previously published regions associated with response inhibition [1] in this sample, but here, we test additional contrasts to measure neural correlates of both response inhibition and error processing. With our large sample, our explorations in this paper combined with the previous publication should prove to be sufficiently powered to find the definitive set or neural correlates of response inhibition and error processing on this task.

2. Methods

2.1. Participants

Participants consisted of 102 healthy adults (49 men) ranging in age from 23 to 52 years (*M* = 33.92, *SD* = 9.64) drawn from the Olin Neuropsychiatry Research Center at the Institute of Living Hartford Hospital and the surrounding community of Hartford, CT via advertisements, presentations at local universities, and word-of-mouth. Seven participants (7%) were left-handed. The sample reflected the ethnic nature of the community: 68% of the sample self-identified as White, 10% as Black/African American, 9% as Hispanic, 8% as Asian, and 6% as Mixed/Other racial heritage. Using the Structured Clinical Interview for the DSM-IV, all participants were free of any history of psychiatric illness (Axis I and II; [46]) and reported no history of psychosis in first-degree relatives. All participants reported normal hearing and normal or corrected to normal visual acuity by contact lenses or MR compatible glasses. Protocols were approved by the Institutional Review Board of Hartford s Hospital and participants provided written informed consent

2.2. Experimental Design

Two scanning runs each comprising 245 visual stimuli were presented to participants using a computer-controlled visual and auditory presentation package. Stimuli were displayed on a rear-projection screen mounted at the rear entrance to the magnet bore and subtended a visual angle of ~3 × 3.5°. Each stimulus appeared for 250 ms in white text within a continuously displayed rectangular fixation box. Participants viewed the screen by means of a mirror system attached to the head coil.

Participants were instructed to respond as quickly and accurately as possible with their right index finger to each presentation of the Go stimulus (the letter X; 412 total trials with the occurrence probability of 0.84). They were instructed to withhold a response to the NoGo stimulus (the letter K; 78 total trials with the occurrence probability of 0.16). Task difficulty could be attributed to the rapid exposure to rare violations of this response set using stimulus letters close in visual similarity. The relatively high probability of targets was necessary to build a pre-potent response set and elicit a sufficient number of errors to justify their

independent examination. Before each run, all participants were encouraged to respond as quickly and accurately as possible. Prior to scanning, participants completed a brief practice session of ~10 trials.

The stimulus onset asynchrony (SOA) between stimuli varied pseudo-randomly between 1000, 2000 and 3000 ms with an average SOA of 1.5 s. No more than three Go stimuli were presented within each consecutive 6 s period. The NoGo stimuli were interspersed among the Go stimuli in a pseudorandom manner subject to three constraints: the minimum SOA between a Go and NoGo stimulus was 1000 ms; the SOA between successive NoGo stimuli was between 8 s and 15 s; and stimuli (both Go and NoGo) had an equal likelihood of occurring at 0, 500 or 1000 ms after the beginning of a 1.5 s acquisition period (TR). By jittering stimulus presentation relative to the acquisition time, the hemodynamic response to the stimuli of interest was sampled effectively at 500 ms intervals.

Behavioral responses were recorded using a commercially available MRI-compatible fiber optic response device (Lightwave Medical, Vancouver, BC). “Hits” were defined as Go (X stimuli) events that were followed by a button press within 1000 ms of stimulus onset. “Misses” were defined as Go events where the participant did not respond within 1000 ms of stimulus onset. “correct rejections” were determined by the absence of a motor response within 1000 ms of the NoGo stimulus. “false alarms” were defined as a motor response following a NoGo stimulus.

2.3. Imaging Parameters

Imaging data were collected on a Siemens Allegra 3T system located at the Olin Neuropsychiatry Research Center, Hartford, CT. Each participant’s head was firmly secured using a custom head holder, and head motion was restricted using a custom cushion inside the head coil. Localizer images were acquired to determine functional image volumes. The echo planar image (EPI) gradient-echo pulse sequence (TR/TE = 1500/28 ms; flip angle = 65°; FOV = 24 × 24 cm; 64 × 64 matrix; 3.4 × 3.4 mm in plane resolution; 5 mm effective slice thickness; 30 total slices) effectively covered the entire brain (150 mm) in 1.5 s. Each of the two runs lasted just over 7 minutes, or 281 scans. A 9 s rest period was included prior to the start of the task in each run to allow for T_1 effects to stabilize. The six initial images from the stabilization period were discarded before post-processing.

2.4. Image Processing

Functional images were reconstructed offline at 16-bit resolution and manually reoriented to approximately the anterior commissure/posterior commissure (AC/PC) plane. Functional image runs were motion corrected using an algorithm based on the principle of M-estimation which reduces the influence of large local intensity changes (INRIAlign; [47, 48]) as implemented in the SPM2 software [49].

A mean functional image volume was constructed for each run from the realigned image volumes. The mean EPI image was normalized to the EPI template. The spatial transformation into standard MNI space was determined using a tailored algorithm with both linear and nonlinear components [50]. The normalization parameters determined for the mean functional volume were then applied to the corresponding functional image volumes

for each participant. The normalized functional images were smoothed with a 9 mm full width at half-maximum (FWHM) Gaussian filter. Event-related responses were modeled using a synthetic hemodynamic response function composed of two gamma functions. The first gamma function modeled the hemodynamic response using a peak latency of 6 s. A term proportional to the derivative of this gamma function was included to allow for small variations in peak latency. The second gamma function and associated derivative was used to model the small "overshoot" of the hemodynamic response on recovery. High-pass (cutoff period 116 s) and low-pass (cutoff period 0.23 s) filters were applied to remove any low- and high-frequency confounds, respectively. A latency variation amplitude-correction method was used to provide a more accurate estimate of hemodynamic response for each condition that controlled for differences between slices in timing and variation across regions in the latency of the hemodynamic response [51].

In addition to the traditional hemodynamic response contrast (beta values for condition A > beta values for condition B), three hemodynamic variants were determined by calculating and comparing the beta values for each contrast: (1) one condition has a large positive response relative to another condition s smaller response of the same direction; (2) one condition has a positive response while the other condition has a negative response, and (3) one condition has a small negative response relative to the other condition s large response of the same direction. In each instance, whole-brain analysis was carried out using *t*-test to identify significant differences. These three response types likely reflect different information processes in the brain and highlight the fact that not all interpretations of traditional contrasts are equal (for discussion, see [1]). Most studies employing fMRI have not focused on the relative directionality of the hemodynamic response but rather only on identifying significant differences, regardless of the variant.

2.5. Data Analytic Strategy

To highlight neural correlates of response inhibition and error processing, first-level general linear models (GLMs) included regressors to model motion (six parameters), hits, misses, correct rejections, and false alarms and their temporal derivatives. For completeness, two additional contrasts were created: 1) Hits were compared to false alarms; 2) correct rejections were compared to false alarms. Contrasts of correct rejections compared to Hits were presented previously [1]. The threshold for all contrasts was $p < .05$, corrected for multiple comparisons using the family-wise error (FWE) correction as implemented in SPM. Additionally, we examined age and sex related effects in these data. No significant correlations with age or sex related differences were observed. As discussed in the companion analysis [1], no regions of interest survived correction in analyses of fast vs slow responders and false alarm error-rates. Finally, d was calculated and correlations were performed with for each contrast (i.e., Hits vs. correct rejections, Hits vs. false alarms, and false alarms vs. correct rejections). None of these correlations proved significant. The fMRI modeling procedure employed here took into consideration the latency related to amplitude differences in hemodynamic response (for full details, see [51]) to ensure the most accurate measurement controlling for latency jitter (as might be found between fast and slow responses to Hits, high and low false alarm error-rates, and differences in d measures). Response time (RT) to Hits and false alarms were included in the first-level SPM models as

parametric modulation. In this parametric model, no derivatives were included. As discussed below, RT to false alarms, but not Hits, was related to BOLD response. Finally, we explored measures of post-error slowing but, as expected based on our specific method, we did not find evidence of post-error slowing in this sample. Participants were instructed to emphasize speed instead of accuracy which increased errors and decreased the likelihood of post-error slowing ([52]. Also, post-error slowing is best induced when stimuli are presented with an SOA of less than 1000 ms ([52]. In the present experiment, our SOA was 1500 ms thus reducing the likelihood of post-error slowing.

3. Results

3.1. Behavioral data

Participants averaged 99% Hits out of total Hits and misses (95% CI upper bound = 99.6%), and the mean percentage of false alarms out of total false alarms and correct rejections was 39% (95% CI upper bound = 41.0%). Average response time (RT) for Hits was 375 ms (*SD* = 85 ms) and false alarms was 345 ms, (*SD* = 69 ms). Age was positively correlated with RT on both Hit ($r = .35$, $p < .001$) and false alarm trials ($r = .33$, $p < .001$). There was no evidence of post-error slowing with mean RT for hits immediately following a false alarm (*M* = 348, *SD*= 50) compared to hits following a correct rejection (*M* = 353, *SD* = 67), did not differ significantly, $t(101) = -1.06$, $p = .29$.

3.2. Imaging data

Error processing—Neural activity in two regions was identified to be negatively related to false alarm response time (inferior frontal gyrus, -51, 6, 18; putamen/lentiform nucleus, -18, -3, 9). These were the only two regions where RT was related to neural activation.

Comparing false alarms with Hits revealed activity in 32 brain regions (Table 1 and Figure 1). Increased positive response was noted for false alarms in ACC (BA 24), superior and medial frontal gyri (BA 6 & 10), and various subcortical regions associated with the basal ganglia, all relative to a smaller positive response for Hits (RED; Figure 1B). A similar pattern was observed for bilateral precentral gyri (BA 4 & 6), bilateral superior temporal gyri (BA 22), bilateral inferior parietal lobule (BA 40), left middle and inferior occipital gryi (BA 18), and cerebellar regions. Activity in the subthalamic nucleus/midbrain was observed. Other regions yielded a positive response for false alarms with a negative response for Hits (GREEN; Figure 1B). These included the bilateral cuneus (BA 17 & 18) and right precuneus (BA 19). Some of these regions have not been commonly observed using the GLM approach (Table 2).

Comparing false alarms with correct rejections revealed 32 areas of activation (Table 3 and Figure 2). Consistent with previous work [3, 37] there was a significant hemodynamic response in both dorsal and rostral ACC (BA 24) extending caudally towards the posterior cingulate cortex and superiorly to include SMA (BA 6), supporting the contribution of ACC to error processing. Activity was also increased in bilateral superior frontal gyri (BA 8 & 10), left medial frontal gryus (BA 9 & 10), bilateral precentral gyri (BA 4 & 6), bilateral superior temporal gyri (BA 22 & 38), right insula (BA 13), right transvers temporal gyrus (BA 42), left supramarginal gyrus (BA 40), right inferior parietal lobe (BA 40), bilateral

postcentral gyri (BA 40), right posterior cingulate (BA 30), and right cerebellum, largely consistent with other reports [11, 14, 16, 32, 33, 53]. Areas of activation less frequently found in studies using GLM-based techniques include the cuneus (BA 30) and precuneus (BA 7 & 31). All regions in this contrast exhibited a positive hemodynamic response for false alarms relative to a smaller positive response to correct rejections except for the cuneus and precuneus, whose responses were positive relative to a negative response for Hits (GREEN; Figure 2B).[1]

Response inhibition—When correct rejections were contrasted with false alarms (Table 4 and Figure 3), seven regions showed significant activation in this condition including bilateral subgenual cingulate (BA 25), right precuneus (BA 7), bilateral middle occipital gyri (BA 18), right inferior parietal lobe (BA 40), and right putamen. Activation in the first two of these areas during successful inhibition has not been consistently observed in previous work of this kind (Table 5; [2, 4]). All regions in this contrast exhibited a positive hemodynamic response for correct rejections relative to a smaller positive response to false alarms. Contrasts of correct rejections compared to Hits were presented previously [1].

4. Discussion

This study represents a complementary, large-scale ($n \geq 100$) event-related fMRI examination of response inhibition and error processing during a challenging Go/NoGo task to Steele et al [1]. By comparing correct rejections and false alarms, response inhibition to a NoGo stimulus was uniquely measured. By comparing false alarms to Hits or correct rejections, unique cognitive processes associated with error-processing were measured. The primary purpose of the current exploration was to identify regions associated with a Go/NoGo task with a large sample (see [42, 43] for discussions of benefits of large sample size in GLM analysis of fMRI).

Response inhibition was explored by comparing correct rejections to false alarms. A large number of brain regions were identified, including bilateral subgenual cingulate, precuneus, bilateral middle occipital gyrus, right inferior parietal lobe, and the right putamen. Combining these results with our previous exploration [1], we have identified a comprehensive set of regions associated with response inhibition commensurate yet extending previous published work [9–11, 14, 21, 54–65]. Also, the bilateral subgenual cingulate was identified here though it is not usually identified in meta-analyses [2, 4].

Error processing, explored by comparing false alarms with Hits or correct rejections, was also associated with neural activity in a large number of brain regions. Regions associated with false alarms compared to Hits include the ACC, SMA, subthalamic nucleus/midbrain, inferior frontal gyrus, anterior frontal cortex, inferior and middle occipital gyri, and the precuneus. Regions associated with false alarms compared to correct rejections include the ACC, superior and medial frontal gyri, and various subcortical regions associated with the basal ganglia, the precentral gyri, superior temporal gyri, insula, inferior parietal lobule,

[1]In two additional analyses, correct rejections and false alarms were also contrasted with their implicit baselines. These analyses yielded activation maps that were largely redundant with correct rejections vs. Hits (previously published [1]) and false alarms vs. Hits. Therefore, the implicit baseline results are not reported.

occipital lobe, left postcentral gyrus, transverse temporal gyrus, cerebellar regions, posterior cingulate, cuneus, precuneus, and right postcentral gyrus. We confirmed the involvement of many regions that had not been consistently found in previous studies using traditional analytic techniques. Tables 2 and 5 summarize the degree of correspondence between the present results and those of similar studies despite occasional differences in baseline. We restrict this comparison to GLM-based fMRI studies of inhibition in healthy adults performing the classical Go/NoGo task (Tables 2 & 5). By using traditional and new hemodynamic variants, we have been able to identify relative activation levels between conditions that allows for a more thorough understanding of the neural correlates of response inhibition and error processing.

Our results also implicated several additional regions including the lateral prefrontal cortex, orbitofrontal gyrus, and temporal gyri. Similar regions have been identified in previous error processing and conflict monitoring research (see [1] for additional response inhibition analyses). Both dorsal and rostral regions of the ACC were identified to be associated with error processing [3] though dorsal activation is thought to contribute to response selection and rostral activation is thought to represent the affective component of error processing [5, 17, 31, 36, 37]. Also, left lateral prefrontal involvement found here replicates previous finding [3, 66, 67]. This finding is consistent with electrophysiological findings showing that left lateral prefrontal cortex lesions result in abnormal behavioral responses and disrupted error-related brain activity [40, 41]. Error trials were associated with hemodynamic response in the inferior frontal gyrus, a region thought to be involved in maintaining response representations and mapping rules [41]. Interestingly, inferior frontal gyrus was negatively correlated with false alarm response time. This effect could be interpreted as a measure of unsuccessful response inhibition and is similar to previous fMRI findings [68, 69]. There is also ERP evidence of greater activation related to faster responding [70]. Overall, this effect could be interpreted as either increase response conflict or error monitoring related to our task instructions that emphasized speed over accuracy. Additional explorations are necessary before firm interpretations are possible. Finally, we identified many of the same regions as Garavan et al., [11, 17] who found that error processing engages not only medial frontal, but a range of other areas, including the inferior parietal lobe, occipital/temporal junction, middle temporal gyrus, and insula.

We also noted significant error-related activity in subcortical regions such as the pons and subthalamic nucleus/midbrain. Here we are one of the first to report subthalamic nucleus/midbrain, part of the basal ganglia, to be activated by error processing. This is interesting considering the basal ganglia is hypothesized to be crucial for error monitoring and for learning from erroneous responses [34]. This hypothesis is supported by previous findings; error-related subcortical engagement has been observed using ICA [32, 33]. Ullsperger and von Cramon [40] found focal lesions to the basal ganglia (putamen and pallidum) and lateral prefrontal regions impaired the ERN, an electrophysiological correlate of error processing. This may be because such lesions impaired cortico–striato–thalamocortical loops running to the ACC. However, to date there have been few functional imaging studies using the GLM to test this hypothesis, and as such, the current study provides one of the first large-scale imaging confirmations of the contribution of the basal ganglia and other subcortical regions

to error processing. In conjunction with previous findings, the current findings add a great deal of support to this hypothesis.

This study yielded several regions not typically observed in previous error processing studies using a GLM approach or in meta-analyses. Particularly novel patterns of activation were observed throughout the occipital cortex such as the inferior and middle occipital gyri and cuneus as well as the fusiform gyrus, a temporal lobe region. This pattern could be attributable to the increased statistical power gained from the greater numbers of errors elicited by this task relative to typical Go/NoGo tasks.

Another goal of the current study was to explore differences in hemodynamic response directionality as we have done previously [1]. Increased activation was noted for false alarms relative to Hits in the ACC, superior and medial gyri, and several temporal and parietal lobe areas (RED; Figure 1B). Similarly, increased activation was noted for false alarms relative to correct rejections in the ACC, superior and medial frontal gyri, and various subcortical regions associated with the basal ganglia, all relative to a smaller positive response for correct rejections (RED; Figure 2B). Other regions yielded activation associated with false alarms that were positive with respect to a negative response for Hits (GREEN; Figure 1B). These regions included cuneus and precuneus. Similar regions yielded activation associated with false alarms that were positive with respect to a negative response for correct rejections (GREEN; Figure 2B). These included the posterior cingulate, cuneus, precuneus, and right postcentral gyrus.

Though the regions plotted in GREEN in Figures 1B and 1B represent activation differences between false alarms and Hits or correct rejections, respectively, these regions may not be associated with error-monitoring directly. For instance, both the cuneus and precuneus have been linked to consciousness, episodic memory retrieval, and the default mode network [71–74] and the observed direction of measured effects with our hemodynamic variants could potentially be explained by these theories. This could be interpreted as only the RED regions, not the GREEN, found in Figures 1B and 2B truly make up a network associated with error processing. By differentiating between the three types of hemodynamic responses within a dataset, investigators can refine their models of response inhibition and error processing. Knowing the directionality of the hemodynamic response can also improve reliability assessments of brain areas that appear to be similarly engaged across multiple study samples and tasks. Future explorations of response inhibition and error processing with such hemodynamic variants are needed before stronger conclusions can be established.

There are some limits to the generalizability of this study. As discussed above, no evidence of post-error slowing was measured in this experiment. As demonstrated by previous work (e.g., [11, 21, 58, 60, 65]), the interpretation of these Go/NoGo results cannot necessarily be expanded to include other forms of response inhibition, such as the inhibition of already initiated motor-responses seen in stop-signal tasks. For example, we have identified, increased activity in striatal regions for correct rejections, a finding supported by previous reports of Go/NoGo tasks [11, 21, 60, 65]. In contrast to this finding, correct rejections measured during a stop-signal task frequently implicate the subthalamic nucleus [19, 59], another region of the basal ganglia. These varied findings could potentially reflect the

different demands of the two inhibition tasks [75]. This is interesting considering the basal ganglia is hypothesized to be crucial for error monitoring and for learning from erroneous responses [34]. This hypothesis is supported by previous findings; error-related subcortical engagement has been observed using ICA [32, 33]. Ullsperger and von Cramon [40] found focal lesions to the basal ganglia (putamen and pallidum) and lateral prefrontal regions impaired the ERN, an electrophysiological correlate of error processing. This may be because such lesions impaired cortico striato thalamocortical loops running to the ACC. However, to date there have been few functional imaging studies using the GLM to test this hypothesis, and as such, the current study provides one of the first large-scale imaging confirmations of the contribution of the basal ganglia and other subcortical regions to error processing. A full understanding of response inhibition and error monitoring must consider variations between tasks at least as much as the convergence commonly emphasized within tasks. Similarly, extrapolation from the error processing measured here compared to other situations when errors occur may not be appropriate. Error processing in this Go/NoGo task may not necessarily be the same as error processing in other tasks that elicit errors (i.e., not all errors are created equal; [76]). Meta-analyses (e.g., [2, 4]) are specifically designed to identify the specific underlying cognitive process across heterogeneous tasks to answer such a global question of response inhibition and error processing. Finally, participant age and sex were not related to our findings. However, these variables have been known to have a moderating influence on how the brain learns to inhibit responses in the Go/NoGo task (e.g., [77]). Future research should consider further testing these variables better isolate their specific contribution to response inhibition and error processing.

Taken together, the current study identified numerous regions that have been inconsistently shown to be engaged in error processing and response inhibition using similar methods. Indeed, no other study has reported engagement of the breadth of regions observed here despite using various baselines. This speaks to the importance of larger samples in imaging studies that employ GLM techniques. We identified 32 regions each when false alarms elicited greater activation than Hits and 32 regions when false alarms elicited greater activation than correct rejections (Table 1 & 2, respectively). Also, we identified seven regions that elicited greater activation to correct rejections than to false alarms (Table 4). This is comparable to the number of regions of interest identified in our previous study response inhibition in a Go/NoGo task [1] and a previous study using 100 participants who completed an auditory oddball task [42]. Though the GLM analysis we performed is one of the large samples of its kind in this area, it is possible that data-driven techniques like ICA may reveal additional error-related changes that do not track cleanly with our GLM model. These data-driven techniques are more robust against Type II errors even with smaller samples [32, 33, 78], and this should be a focus of future research of this kind. Also, event-related potentials (ERP) have often been used to identify response inhibition processes (e.g., [12, 18, 20, 79]) and error processing (e.g., [34, 39, 76]). Combining ERPs and fMRI findings with a unique ICA analysis [80] could help further elucidate the time course and spatial location of neural activity associated with response inhibition and error processing.

5. Conclusions

In summary, the results presented here represent one of the largest imaging investigations of response inhibition and error processing in a healthy sample conducted to date. Participants were presented with a fast-paced Go/NoGo task. We identified a substantial number of regions specific to response inhibition and error-monitoring providing a thorough description of the networks involved in Go/NoGo tasks. When combined with our previous exploration of response inhibition [1], we have identified a comprehensive set of regions associated with response inhibition and error processing. Finally, we highlighted the advantage of analyzing additional hemodynamic responses to better isolate neural correlates of response inhibition and error processing.

Acknowledgments

The authors thank Craig Bennett, Matthew Shane, J. Michael Maurer, Lora Cope, members of the Olin Neuropsychiatry Research Center, and members of the Mind Research Network. This research was supported in part by grants from the National Institute of Mental Health: 1 R01 MH070539-01 (PI: Kiehl), 1 R01 MH071896-01 (PI: Kiehl), RO1 DA020709 (PI: Pearlson), and P50-AA12870-05 (PI for Project 4: Pearlson).

References

1. Steele VR, Aharoni E, Munro GE, Calhoun VD, Nyalakanti P, Stevens MC, et al. A large scale (N = 102) functional neuroimaging study of response inhibition in a Go/NoGo task. Behav Brain Res. 2013; 256:529–36. [PubMed: 23756137]
2. Niendam TA, Laird AR, Ray KL, Dean YM, Glahn DC, Carter CS. Meta-analytic evidence for a superordinate cognitive control network subserving diverse executive functions. Cogn Affect Behav Neurosci. 2012; 12:241–68. [PubMed: 22282036]
3. Kiehl KA, Liddle PF, Hopfinger JB. Error processing and the rostral anterior cingulate: An event-related fMRI study. Psychophysiology. 2000; 37:216–23. [PubMed: 10731771]
4. Simmonds DJ, Pekar JJ, Mostofsky SH. Meta-analysis of Go/No-go tasks demonstrating that fMRI activation associated with response inhibition is task-dependent. Neuropsychologia. 2008; 46:224–32. [PubMed: 17850833]
5. Braver TS, Barch DM, Gray JR, Molfese DL, Snyder A. Anterior cingulate cortex and response conflict: Effects of frequency, inhibition, and errors. Cereb Cortex. 2001; 11:825–36. [PubMed: 11532888]
6. Horn NR, Dolan M, Elliott R, Deakin JFW, Woodruff PWR. Response inhibition and impulsivity: An fMRI study. Neuropsychologia. 2003; 41:1959–66. [PubMed: 14572528]
7. Liddle PF, Kiehl KA, Smith AM. Event-related fMRI study of response inhibition. Hum Brain Mapp. 2001; 12:100–9. [PubMed: 11169874]
8. Schulz KP, Fan J, Tang CY, Newcorn JH, Buchsbaum MS, Cheung AM, et al. Response inhibition in adolescents diagnosed with attention deficit hyperactivity disorder during childhood: An event-related fMRI study. American Journal of Psychiatry. 2004; 161:1650–7. [PubMed: 15337656]
9. Aron AR, Robbins TW, Poldrack RA. Inhibition and the right inferior frontal cortex. Trends Cogn Sci. 2004; 8:170–7. [PubMed: 15050513]
10. Garavan H, Ross TJ, Stein EA. Right hemispheric dominance of inhibitory control: An event-related functional MRI study. Proc Natl Acad Sci U S A. 1999; 96:8301–6. [PubMed: 10393989]
11. Garavan H, Ross TJ, Murphy K, Roche RAP, Stein EA. Dissociable executive functions in the dynamic control of behavior: Inhibition, error detection, and correction. Neuroimage. 2002; 17:1820–9. [PubMed: 12498755]
12. Mathalon DH, Whitfield SL, Ford JM. Anatomy of an error: ERP and fMRI. Biol Psychol. 2003; 64:119–41. [PubMed: 14602358]

13. McNab F, Leroux G, Strand F, Thorell L, Bergman S, Klingberg T. Common and unique components of inhibition and working memory: An fMRI, within-subjects investigation. Neuropsychologia. 2008; 46:2668–82. [PubMed: 18573510]
14. Menon V, Adleman NE, White CD, Glover GH, Reiss AL. Error-related brain activation during a Go/NoGo response inhibition task. Hum Brain Mapp. 2001; 12:131–43. [PubMed: 11170305]
15. Wager TD, Sylvester CY, Lacey SC, Nee DE, Franklin M, Jonides J. Common and unique components of response inhibition revealed by fMRI. Neuroimage. 2005; 27:323–40. [PubMed: 16019232]
16. Mostofsky SH, Schafer JGB, Abrams MT, Goldberg MC, Flower AA, Boyce A, et al. fMRI evidence that the neural basis of response inhibition is task-dependent. Cognitive Brain Research. 2003; 17:419–30. [PubMed: 12880912]
17. Garavan H, Ross TJ, Kaufman J, Stein EA. A midline dissociation between error-processing and response-conflict monitoring. Neuroimage. 2003; 20:1132–9. [PubMed: 14568482]
18. Tian Y, Yao D. A study on the neural mechanism of inhibition of return by the event-related potential in the Go/NoGo task. Biol Psychol. 2008; 79:171–8. [PubMed: 18524452]
19. Aron AR. The neural basis of inhibition in cognitive control. The Neuroscientist. 2007; 13:214–28. [PubMed: 17519365]
20. Bekker EM, Kenemans JL, Verbaten MN. Source analysis of the N2 in a cued Go/NoGo task. Cognitive Brain Research. 2005; 22:221–31. [PubMed: 15653295]
21. Garavan H, Hester R, Murphy K, Fassbender C, Kelly C. Individual differences in the functional neuroanatomy of inhibitory control. Brain Res. 2006; 1105:130–42. [PubMed: 16650836]
22. Braver TS, Barch DM, Gray JR, Molfese DL, Snyder A. Anterior cingulate cortex and response conflict: Effects of frequency, inhibition and errors. Cerebral Cortex. 2001; 11:825–36. [PubMed: 11532888]
23. Garavan H, Ross TJ, Murphy K, Roche RAP, Stein EA. Dissociable executive functions in the dynamic control of behavior: Inhibition, error detection, and correction. NeuroImage. 2002; 17:1820–9. [PubMed: 12498755]
24. Horn NR, Dolan M, Deakin JFW, Woodruff PWR. Response inhibition and impulsivity: An fMRI study. Neuropsychologia. 2003; 41:1959–66. [PubMed: 14572528]
25. Kiehl KA, Smith AM, Hare RD, Liddle PF. An event-related potential investigation of response inhibition in schizophrenia and psychopathy. Biological Psychiatry. 2000; 48:210–21. [PubMed: 10924664]
26. Liddle PF, Kiehl KA, Smith AM. Event-related fMRI study of response inhibition. Hum Brain Mapp. 2001; 12:100–9. [PubMed: 11169874]
27. Menon V, Adleman NE, White CD, Glover GH, Reiss AL. Error-related brain activation during a Go/No-go response inhibition task. Human Brain Mapping. 2001; 12:131–43. [PubMed: 11170305]
28. Holroyd CB, Coles MGH. The neural basis of human error-processing: Reinforcement learning, dopamine and the error-related negativity. Psychological Review. 2002; 109:679–709. [PubMed: 12374324]
29. Carter CS, Braver TS, Barch DM, Botvinick M, Noll D, Cohen JD. Anterior cingulate cortex, error detection, and the online monitoring of performance. Science. 1998; 280:747–9. [PubMed: 9563953]
30. Holroyd CB, Nieuwenhuis S, Yeung N, Nystrom L, Mars RB, Coles MG, et al. Dorsal anterior cingulate cortex shows fMRI response to internal and external error signals. Nat Neurosci. 2004; 7:497–8. [PubMed: 15097995]
31. Ullsperger M, von Cramon DY. Subprocesses of performance monitoring: A dissociation of error processing and response competition revealed by event-related fMRI and ERPs. Neuroimage. 2001; 14:1387–401. [PubMed: 11707094]
32. Stevens MC, Kiehl KA, Pearlson GD, Calhoun VD. Brain network dynamics during error commission. Hum Brain Mapp. 2009; 30:24–37. [PubMed: 17979124]
33. Stevens MC, Kiehl KA, Pearlson GD, Calhoun VD. Functional neural networks underlying response inhibition in adolescents and adults. Behav Brain Res. 2007; 181:12–22. [PubMed: 17467816]

34. Holroyd CB, Coles MGH. The neural basis of human error processing: Reinforcement learning, dopamine, and the error-related negativity. Psychological Review. 2002; 109:679–709. [PubMed: 12374324]
35. Edwards BG, Calhoun VD, Kiehl KA. Joint ICA of ERP and fMRI during error-monitoring. Neuroimage. 2012; 59:1896–903. [PubMed: 21930218]
36. Devinsky O, Morrell MJ, Vogt BA. Contributions of anterior cingulate to behaviour. Brain. 1995; 188:279–306. [PubMed: 7895011]
37. Polli FE, Barton JJ, Cain MS, Thakkar KN, Rauch SL, Manoach DS. Rostral and dorsal anterior cingulate cortex make dissociable contributions during antisaccade error commission. Proc Natl Acad Sci U S A. 2005; 102:15700–5. [PubMed: 16227444]
38. Falkenstein M, Hielscher H, Dziobeck I, Schwarzenau P, Hoorman J, Sundermann B, et al. Action monitoring, error detection, and the basal ganglia: An ERP study. Neuroreport. 2001; 12:157–61. [PubMed: 11201078]
39. Gehring WJ, Knight RT. Prefrontal-cingulate interactions in action monitoring. Nat Neurosci. 2000; 3:516–20. [PubMed: 10769394]
40. Ullsperger M, von Cramon DY. The role of intact frontostriatal circuits in error processing. Journal of Cognitive Neuroscience. 2006; 18:651–64. [PubMed: 16768367]
41. Ullsperger M, von Cramon DY, Müller NG. Interactions of frontal cortical lesions with error processing: Evidence from event-related brain potentials. Neuropsychology. 2002; 16:548–61. [PubMed: 12382993]
42. Kiehl KA, Stevens MC, Laurens KR, Pearlson G, Calhoun VD, Liddle PF. An adaptive reflexive processing model of neurocognitive function: Supporting evidence from a large scale (n = 100) fMRI study of an auditory oddball task. Neuroimage. 2005; 25:899–915. [PubMed: 15808990]
43. Murphy K, Garavan H. An empirical investigation into the number of subjects required for an event-related fMRI study. Neuroimage. 2004; 22:879–85. [PubMed: 15193618]
44. Bellgrove MA, Hester R, Garavan H. The functional neuroanatomical correlates of response variability: Evidence from a response inhibition task. Neuropsychologia. 2004; 42:1910–6. [PubMed: 15381021]
45. Rubia K, Smith AB, Woolley J, Nosarti C, Heyman I, Taylor E, et al. Progressive increase of frontostriatal brain activation from childhood to adulthood during event-related tasks of cognitive control. Hum Brain Mapp. 2006; 27:973–93. [PubMed: 16683265]
46. First, MB.; Spitzer, RL.; Gibbon, MWJB.; Williams, JBW. Structured clinical interview for DSM-IV axis I (SCID-I), clinician version. Washington DC: American Psychiatric Press; 1997.
47. Freire L, Mangin JF. Motion correction algorithms may create spurious brain activations in the absence of subject motion. Neuroimage. 2001; 14:709–22. [PubMed: 11506543]
48. Freire L, Roche A, Mangin JF. What is the best similarity measure for motion correction in fMRI time series? IEEE Transactions on Medical Imaging. 2002; 21:470–84. [PubMed: 12071618]
49. Wellcome Trust Centre for Neuroimaging UCL.
50. Friston KJ, Holmes AP, Worsley KJ, Poline J-P, Frith CD, Frackowiak RSJ. Statistical parametric maps in functional imaging: A general linear approach. Hum Brain Mapp. 1994; 2:189–210.
51. Calhoun VD, Stevens MC, Pearlson GD, Kiehl KA. fMRI analysis with the general linear model: Removal of latency-induced amplitude bias by incorporation of hemodynamic derivative terms. Neuroimage. 2004; 22:252–7. [PubMed: 15110015]
52. Danielmeier C, Ullsperger M. Post-error adjustments. Front Psychol. 2011; 2:1–10. [PubMed: 21713130]
53. Braet W, Johnson KA, Tobin CT, Acheson R, Bellgrove MA, Robertson IH, et al. Functional developmental changes underlying response inhibition and error-detection processes. Neuropsychologia. 2009; 47:3143–51. [PubMed: 19651151]
54. Hirose S, Chikazoe J, Jimura K, Yamashita K, Miyashita Y, Konishi S. Sub-centimeter scale functional organization in human inferior frontal gyrus. Neuroimage. 2009; 47:442–50. [PubMed: 19442752]
55. Chambers CD, Bellgrove MA, Gould IC, English T, Garavan H, McNaught E, et al. Dissociable mechanisms of cognitive control in prefrontal and premotor cortex. J Neurophysiol. 2007; 98:3638–47. [PubMed: 17942624]

56. Chambers CD, Garavan H, Bellgrove MA. Insights into the neural basis of response inhibition from cognitive and clinical neuroscience. Neurosci Biobehav Rev. 2009; 33:631–46. [PubMed: 18835296]
57. Chikazoe J, Konishi S, Asari T, Jimura K, Miyashita Y. Activation of right inferior frontal gyrus during response inhibition across response modalities. Journal of Cognitive Neuroscience. 2007; 19:69–80. [PubMed: 17214564]
58. Aron AR, Durston S, Eagle DM, Logan GD, Stinear CM, Stuphorn V. Converging evidence for a fronto-basal-ganglia network for inhibitory control of action and cognition. The Journal of Neuroscience. 2007; 27:11860–4. [PubMed: 17978025]
59. Aron AR, Poldrack RA. Cortical and subcortical contributions to stop signal response inhibition: Role of the subthalamic nucleus. The Journal of Neuroscience. 2006; 26:2424–33. [PubMed: 16510720]
60. Durston S, Thomas KM, Yang Y, Ulug AM, Zimmerman RD, Casey BJ. A neural basis for the development of inhibitory control. Dev Sci. 2002; 5:F9–F16.
61. Casey BJ, Castellanos FX, Giedd JE, Marsh WL, Hamburger SD, Schubert AB, et al. Implication of the right frontostriatal circuitry in response inhibition and attention-deficit/hyperactivity disorder. J Am Acad Child Adolesc Psychiatry. 1997; 36:374–83. [PubMed: 9055518]
62. Gauggel S, Rieger M, Feghoff TA. Inhibition of ongoing responses in patients with Parkinson's disease. Journal of Neurology, Neurosurgery & Psychiatry. 2004; 75:539–44.
63. Rieger M, Gauggel S, Burmeister K. Inhibition of ongoing responses following frontal, nonfrontal, and basal ganglia lesions. Neuropsychology. 2003; 17:272–82. [PubMed: 12803433]
64. Thoma P, Koch B, Heyder K, Schwarz M, Daum I. Subcortical contributions to multitasking and response inhibition. Behav Brain Res. 2008; 194:214–22. [PubMed: 18692526]
65. Fassbender C, Simoes-Franklin C, Murphy K, Hester R, Meaney J, Robertson IH, et al. The role of a right fronto-parietal network in cognitive control. Journal of Psychophysiology. 2006; 20:286–96.
66. Kerns JG, Cohen JD, MacDonald AW, Cho RY, Stenger VA, Carter CS. Anterior cingulate conflict monitoring and adjustments in control. Science. 2004; 303:1023–6. [PubMed: 14963333]
67. King JA, Korb FM, von Cramon DY, Ullsperger M. Post-error behavioral adjustments are facilitated by activation and suppression of task-relevant and task-irrelevant information processing. The Journal of Neuroscience. 2010; 30:12759–69. [PubMed: 20861380]
68. Ramautar JR, Slagter HA, Kok A, Ridderinkhof KR. Probability effects in the stop-signal paradigm: The insula and the significance of failed inhibition. Brain Res. 2006; 1105:143–54. [PubMed: 16616048]
69. Hester R, Fassbender C, Garavan H. Individual differences in error processing: A review and reanalysis of three event-related fMRI sudies using the go/nogo task. Cereb Cortex. 2004; 14:986–94. [PubMed: 15115734]
70. de Bruijn ER, Miedl SF, Bekkering H. Fast responders have blinders on: ERP correlates of response inhibition in competition. Cortex. 2008; 44:580–6. [PubMed: 18387590]
71. Cavanna AE. The precuneus and consciousness. CNS Spectrums. 2007; 12:545–52. [PubMed: 17603406]
72. Cavanna AE, Trimble MR. The precuneus: A review of its functional anatomy and behavioural correlates. Brain. 2006; 129:564–83. [PubMed: 16399806]
73. Shulman GL, Fiez JA, Corbetta M, Buckner RL, Miezin FM, Raichle ME, et al. Common blood flow changes across visual tasks: II. Decreases in cerebral cortex. Journal of Cognitive Neuroscience. 1997; 9:648–63. [PubMed: 23965122]
74. Wagner AD, Shannon BJ, Kahn I, Buckner RL. Parietal lobe contributions to episodic memory deficits. Trends Cogn Sci. 2005; 9:445–53. [PubMed: 16054861]
75. Aron AR. From reactive to proactive and selective control: Developing a richer model for stopping inappropriate responses. Biol Psychiatry. 2011; 69:55–68. [PubMed: 20970778]
76. Hajcak G, Moser JS, Yeung N, Simons RF. On the ERN and the significance of errors. Psychophysiology. 2005; 42:151–60. [PubMed: 15787852]

77. Nielson KA, Langenecker SA, Ross TJ, Garavan H, Rao SM, Stein EA. Comparability of functional MRI response in young and old during inhibition. Neuroreport. 2004; 15:129–33. [PubMed: 15106844]

78. Calhoun VD, Maciejewski PK, Pearlson GD, Kiehl KA. Temporal lobe and "default" hemodynamic brain modes discriminate between schizophrenia and bipolar disorder. Hum Brain Mapp. 2008; 29:1265–75. [PubMed: 17894392]

79. Bokura H, Yamaguchi S, Kobayashi S. Electrophysiological correlates for response inhibition in a Go/NoGo task. Clinical Neurophysiology. 2001; 112:2224–32. [PubMed: 11738192]

80. Calhoun VD, Adali T, Pearlson GD, Kiehl KA. Neuronal chronometry of target detection: Fusion of hemodynamic and event-related potential data. Neuroimage. 2006; 30:544–53. [PubMed: 16246587]

Highlights

- We examine error processing in a large scale fMRI study
- We identify a comprehensive network associated with error processing
- New regions are shown to be engaged in error processing
- Hemodynamic variants allowed for specificity in the underlying neural mechanisms

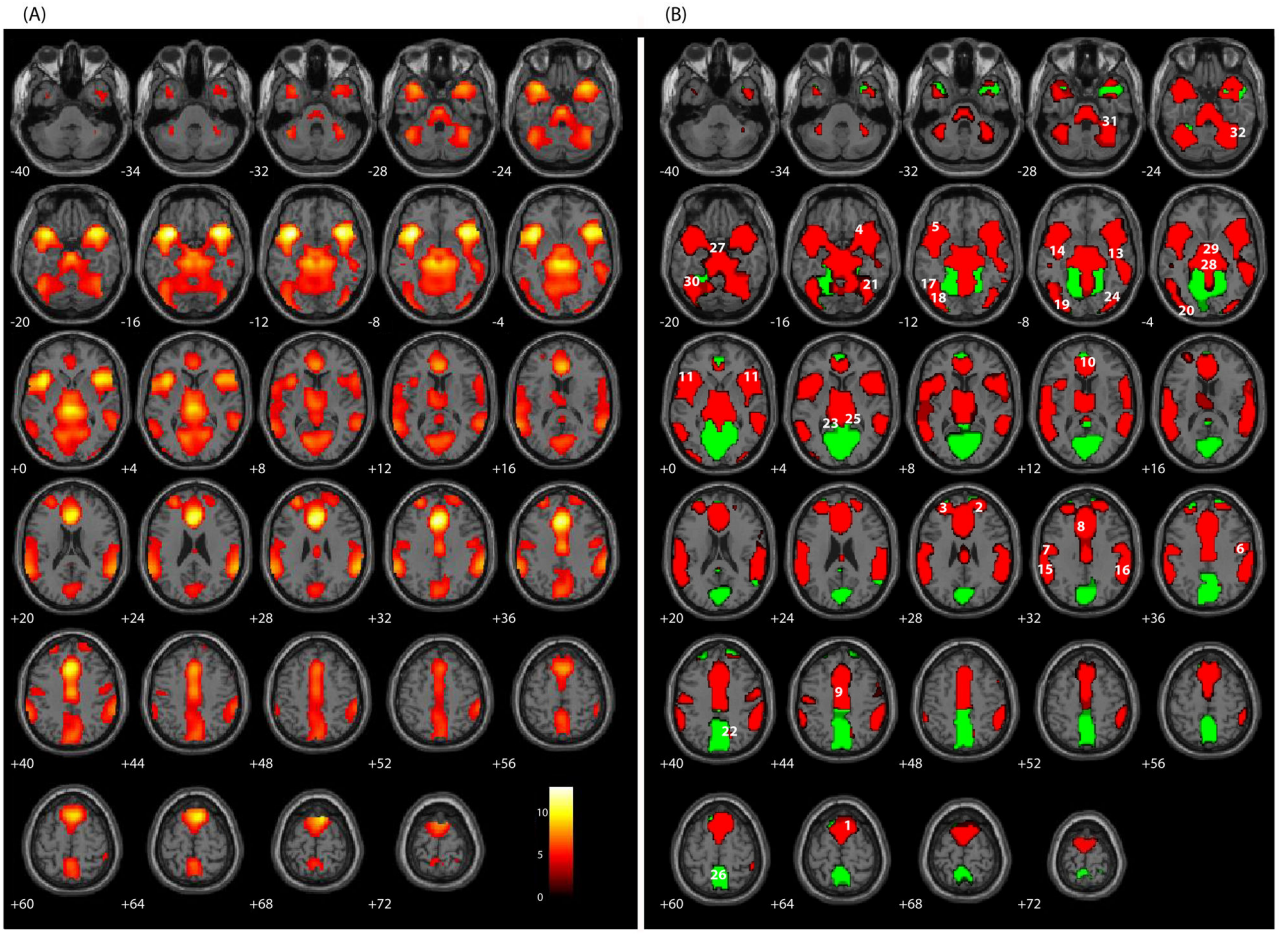

Figure 1.

SPM axial slices of areas of significant activation ($p < .05$, corrected for multiple comparisons) for false alarms relative to Hits for the sample of 102 participants. (A) A traditional, omnibus analysis comparing false alarms and Hits. (B) RED: false alarms have as a large positive response relative to the Hit condition s smaller response of the same direction. GREEN: false alarms have a positive response while Hits has a negative response. BLUE: false alarms have a small negative response relative to the Hit condition s large response of the same direction. Numeric labels denote significant regions of activation anatomically labeled in Table 1.

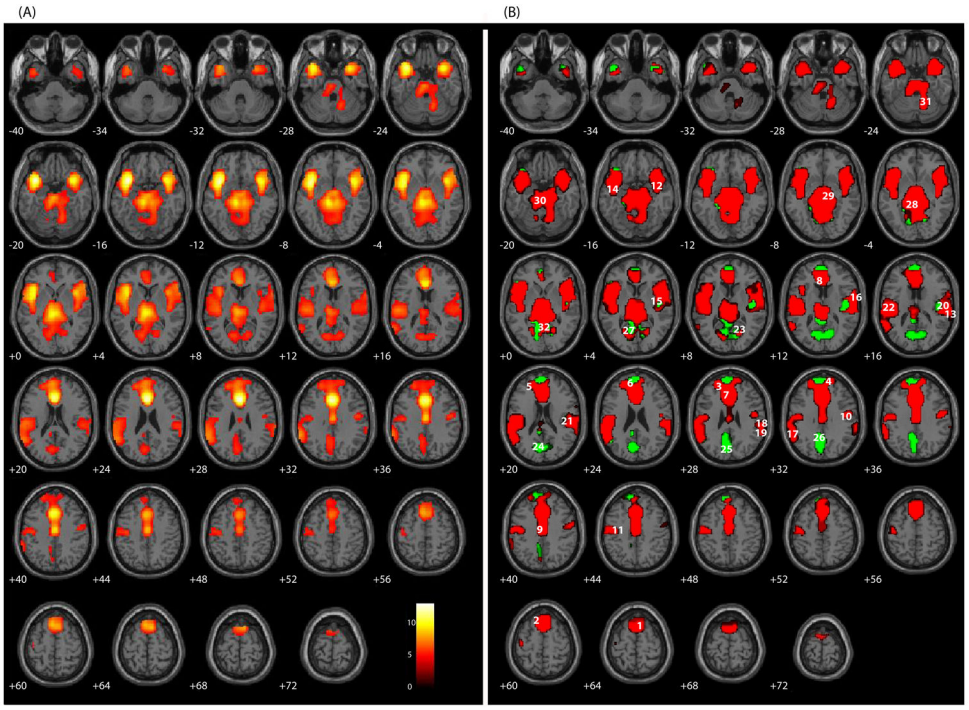

Figure 2.

SPM axial slices of areas of significant activation ($p < .05$, corrected for multiple comparisons) for false alarms relative to correct rejections for the sample of 102 participants. (A) A traditional, omnibus analysis comparing false alarms and correct rejections. (B) RED: false alarms have as a large positive response relative to the correct rejection s smaller response of the same direction. GREEN: false alarms have a positive response while correct rejections havea negative response. BLUE: false alarms have a small negative response relative to the correct rejection s large response of the same direction. Numeric labels denote significant regions of activation anatomically labeled in Table 3.

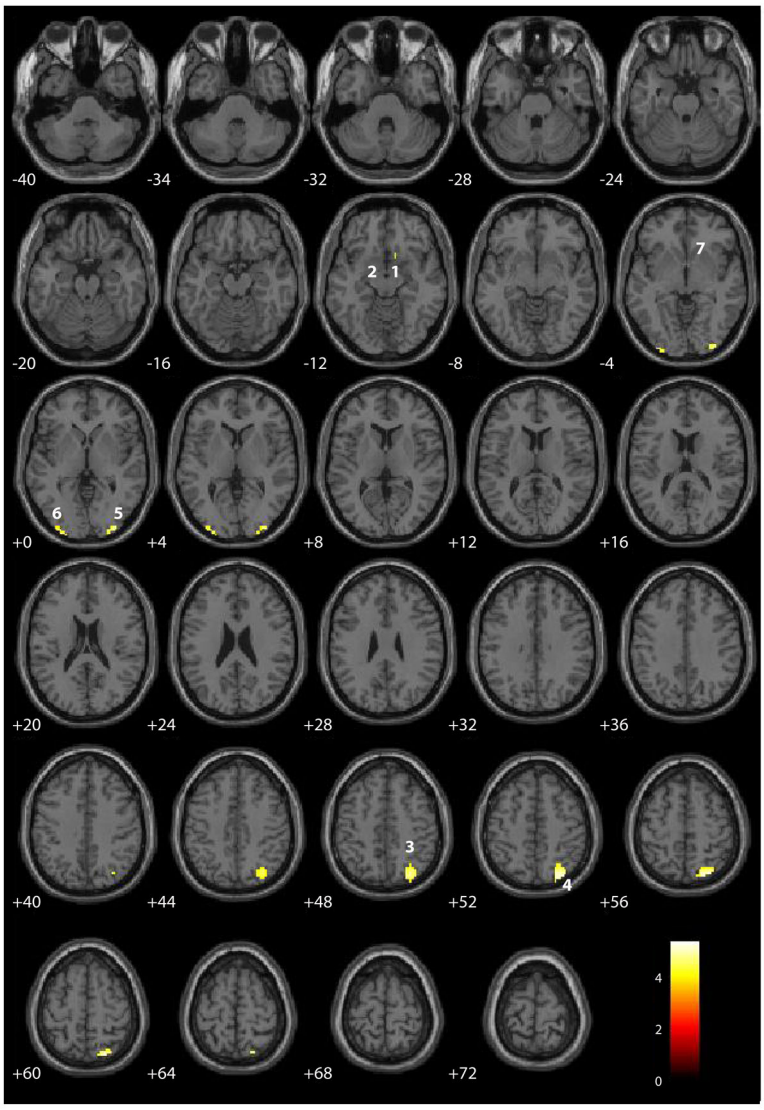

Figure 3.

SPM axial slices of areas of significant activation ($p < .05$, corrected for multiple comparisons) for correct rejections relative to false alarms for the sample of 102 participants. Using the hemodynamic variants, all regions identified in the traditional contrast exhibited a positive hemodynamic response of correct rejections relative to a smaller positive response to false alarms. Numeric labels denote significant regions of activation anatomically labeled in Table 4.

Table 1

Summary of the *t*-scores and the 32 regions of interest extracted from a traditional hemodynamic response analysis of false alarms vs. Hits for the total sample (n = 102). Using the hemodynamic variants, all regions identified in the traditional contrast exhibited a positive hemodynamic response of false alarms relative to a smaller positive response to Hits. In the cuneus, the false alarm response was positive relative to a negative response in Hits. Eta squared is also presented as an account for BOLD signal variance assumed within each ROI.

	Location	*t*-score	*X*	*y*	*z*	BA	η^2
	Frontal Lobe						
1	R Superior Frontal Gyrus	10.99 ****	9	18	66	6	.55
2	R Superior Frontal Gyrus	6.35 ****	24	54	30	10	.29
3	L Superior Frontal Gyrus	8.07 ****	−27	51	30	10	.39
4	R Inferior Frontal Gyrus	13.61 ****	36	18	−15	47	.65
5	L Inferior Frontal Gyrus	14.12 ****	−36	15	−12	47	.66
6	R Precentral Gyrus	5.48 ***	48	−9	36	6	.25
7	L Precentral Gyrus	5.16 **	−51	−12	33	4	.21
8	L Anterior Cingulate Cortex	13.38 ****	−3	24	33	24	.64
9	L Anterior Cingulate Cortex	9.15 ****	0	−12	42	24	.45
10	R Anterior Cingulate Cortex	8.02 *	6	33	12	24	.36
11	Bi Anterior Frontal Cortex	9.6 *	±36	15	0	11	−.40 +.30
	Temporal Lobe						
12	L Superior Temporal Gyrus	8.53 ****	−63	−51	18	22	.42
13	R Middle Temporal Gyrus	7.11 ****	54	−33	−6	21	.33
14	L Middle Temporal Gyrus	4.35 *	−54	−30	−9	21	.16
	Parietal Lobe						
15	L Inferior Parietal Lobule	8.74 ****	−63	−45	30	40	.43
16	R Inferior Parietal Lobule	9.45 ****	63	−42	30	40	.47
	Occipital Lobe						
17	L Middle Occipital Gyrus	7.02 ****	−42	−87	−12	18	.33
18	L Middle Occipital Gyrus	6.99 ****	−45	−81	−12	18	.33

	Location	*t*-score	*X*	*y*	*z*	BA	η^2
19	L Inferior Occipital Gyrus	6.68 ****	−36	−93	−9	18	.31
20	L Inferior Occipital Gyrus	6.34 ****	−33	−96	−6	18	.29
21	R Fusiform	7.08 ****	45	−75	−18	18	.33
22	R Precuneus	7.37 ****	6	−75	42	19	.35
23	L Cuneus	8.12 ****	−12	−72	6	7	.40
24	R Inferior Occipital Gyrus	6.82 ****	42	−87	−9	30	.32
25	R Cuneus/Lingual Gyrus	7.39 ****	15	−66	3	18	.35
26	Intrahemispheric	7.2 ****	0	−54	60	18	.34
	Subcortical						
27	Midbrain (Pons)	9.17 ****	0	−21	−21	NA	.45
28	L Midbrain (Brainstem)	11.38 ****	−3	−30	−3	NA	.56
29	R Subthalamic Nucleus (Midbrain)	7.44 ****	3	−9	−3	NA	.35
	Cerebellum						
30	L Cerebellum (Declive)	7.71 ****	−42	−63	−21	NA	.37
31	R Cerebellum (Culmen)	7.54 ****	36	−51	−27	NA	.36
32	R Cerebellum (Declive)	7.56 ****	39	−57	−24	NA	.36

* *p* .05;

** *p* .01;

*** *p* .001;

**** *p* .0001 corrected for multiple comparisons.

Table 2

Presented here, a comparison of studies where general linear model-based fMRI analysis was used to analyze error processing in healthy adults performing a simple Go/NoGo task. The sample size, baseline, and regions engaged during error processing across these eight fMRI studies employing a simple Go/NoGo task are presented.

			FRONTAL						TEMPORAL				PARIETAL					OCCIPITAL				SUBCORTICAL				CEREBELLAR
Publication	**Sample Size**	**Baseline**	**ACC**	**Cingulate Gy**	**Sup Front Gy**	**Med Front Gy**	**Inf Front Gy**	**Precen Gy**	**Sup Temp Gy**	**Mid Temp Gy**	**Trans Temp Gy**	**Insula**	**Inf Par Lobe**	**Post-cent Gy**	**Supra-mar Gy**	**Post Cing**	**Precun**	**Inf Occ Gy**	**Mid Occ Gy**	**Cuneus**	**Fusi-form Gy**	**Sub-thal Nuc**	**Pons**	**Mid Brain**	**Mam-mil Body**	**Cerebellum**
Errors of Commission																										
Current ($p < .05$)	102	CR & Hits	x	x	x	x	x	x	x	x	x	x	x	x	x	x	x	x	x	x	x	x	x	x	x	x
Magno et al., 2006 ($p < .05$) [80]	19	CR	x	x								x														
Hester et al., 2005 ($p < .05$) [81]	15	Unaware FA	x		x		x		x				x													
Garavan et al., 2003 ($p < .01$) [16]	16	CR	x	x	x					x																
Mathalon et al., 2003 ($p < .05$) [10]	10	Hits	x	x	x	x	x		x			x	x										x	x		x
Garavan et al., 2002 ($p < .05$) [8]	14	CR	x	x		x		x				x	x													
Menon et al., 2001 ($p < .05$) [12]	14	CR	x									x					x									
Kiehl et al., 2000 ($p < .05$) [15]	14	Implicit & CR	x			x																				

Table 3

Summary of the *t*-scores and the 32 regions of interest extracted from a traditional hemodynamic response analysis of false alarms vs. correct rejections for the total sample (n = 102). Using the hemodynamic variants, all regions identified in the traditional contrast exhibited a positive hemodynamic response of false alarms relative to a smaller positive response to correct rejections except for the posterior cingulate, cuneus, precuneus, and right postcentral gyrus, where false alarms positive relative to a negative response in correct rejections. Eta squared is also presented as an account for BOLD signal variance assumed within each ROI.

	Location	*t*-score	*X*	*y*	*z*	BA	η^2
	Frontal Lobe						
1	R Superior Frontal Gyrus	7.94 ***	9	18	63	8	.38
2	L Superior Frontal Gyrus	7.98 ***	−3	21	60	8	.38
3	L Superior Frontal Gyrus	6.1 ***	−21	48	27	10	.28
4	L Superior Frontal Gyrus	5.29 **	18	57	30	10	.22
5	L Medial Frontal Gyrus	7.14 ***	−6	51	18	10	.34
6	L Medial Frontal Gyrus	7.15 ***	−3	54	21	9	.34
7	Anterior Cingulate	11.88 ***	0	24	27	24	.58
8	Anterior Cingulate	7.61 *	0	27	12	24	.29
9	Cingulate Gyrus	8.94 ***	0	−12	39	24	.45
10	R Precentral Gyrus	5.66 ***	48	−9	33	6	.24
11	L Precentral Gyrus	5.69 ***	−39	−18	45	4	.25
	Temporal Lobe						
12	R Superior Temporal Gyrus/Insula	9.93 ***	36	12	−18	38	.59
13	R Superior Temporal Gyrus	4.54 *	69	−39	15	22	.18
14	L Superior Temporal Gyrus/Insula	12.15 ***	−36	12	−18	38	.49
15	R Insula (posterior)	6.09 ***	42	−15	3	13	.27
16	R Transverse Temporal Gyrus	5.35 **	63	−15	12	42	.23
17	L Supramarginal Gyrus	7.23 ***	−63	−45	30	40	.35
	Parietal Lobe						
18	R Inferior Parietal Lobe	5.72 ***	69	−30	27	40	.25

	Location	*t*-score	*X*	*y*	*z*	BA	η^2
19	R Inferior Parietal Lobe	5.69 ***	66	−42	27	40	.25
20	R Postcentral Gyrus	5.47 ***	54	−24	18	40	.24
21	R Postcentral Gyrus	5.46 ***	57	−27	21	40	.24
22	L Postcentral Gyrus	6.77 ***	−54	−21	15	40	.32
23	R Posterior Cingulate	5.3 **	15	−69	9	30	.22
	Occipital Lobe						
24	L Precuneus	5.36 ***	−6	−72	21	31	.23
25	L Precuneus	5.34 **	−6	−72	27	31	.23
26	L Precuneus	5.48 ***	−6	−60	33	7	.24
27	L Cuneus	5.79 ***	−12	−69	6	30	.24
	Subcortical						
28	L Midbrain	9.62 ***	−6	−30	−3	NA	.47
29	R Mammillary Body	7.23 ***	6	−12	−9	NA	.34
30	L Midbrain	7.88 ***	−3	−21	−18	NA	.38
	Cerebellum						
31	R Cerebellum (Dentate)	5.93 ***	15	−60	−24	NA	.26
32	Interhemispheric	5.54 ***	−3	−57	0	18	.23

* *p* .05;

** *p* .01;

*** *p* .001;

**** *p* .0001 corrected for multiple comparisons.

Table 4

Summary of the *t*-scores and the seven regions of interest extracted from a traditional hemodynamic response analysis of correct rejections vs. false alarms for the total sample (n = 102). Using the hemodynamic variants, all regions identified in the traditional contrast exhibited a positive hemodynamic response of correct rejections relative to a smaller positive response to false alarms. Eta squared is also presented as an account for BOLD signal variance assumed within each ROI.

	Location	*t*-score	*X*	*y*	*z*	BA	η^2
	Frontal Lobe						
1	R Subgenual Cingulate	4.28 **	12	12	−12	25	.16
2	L Subgenual Cingulate	4.11 **	−12	15	−15	25	.15
	Parietal Lobe						
3	R Inferior Parietal Lobule	4.04 *	33	−54	48	40	.14
4	R Precuneus	5.75 ***	30	−75	54	7	.24
	Occipital Lobe						
5	R Middle Occipital Gyrus	5.27 ***	33	−96	0	18	.22
6	L Middle Occipital Gyrus	5.03 **	−30	−99	0	18	.21
	Subcortical						
7	R Putamen	4.20 **	24	6	−3	NA	.15

* p .05;

** p .01;

*** p .001 corrected for multiple comparisons.

Table 5

Presented here, a comparison of studies where general linear model-based fMRI analysis was used to analyze response inhibition in healthy adults performing a simple Go/NoGo task. The sample size, baseline, and regions engaged during successful response inhibition across these 15 fMRI studies employing a simple Go/NoGo task are presented. This table also appears in Steele et al. [1].

			FRONTAL				TEMPORAL				PARIETAL		OCCIPITAL			SUBCORTICAL			CEREBELLAR
Publication	**Sample Size**	**Baseline**	**ACC**	**Sup Front Gy**	**Mid Front Gy**	**Inf Front Gy**	**Sup Temp Gy**	**Mid Temp Gy**	**Supra-mar Gy**	**Ins**	**Inf Par Lobe**	**Precun**	**Inf Occ Gy**	**Cuneus**	**Fusi-form Gy**	**Lingual Gy**	**Mid brain**	**Lenti Nuc**	**Cerebellum**
Inhibition																			
Steele et al., 2013 ($p < .05$)	102	FA & Hits	x	x	x	x	x	x	x	x	x	x	x	x	x	x	x	x	x
Chikazoe et al., 2009 ($p < .05$)	25	Hits		x	x	x	x				x	x						x	x
McNab et al., 2008 ($p < .001$)	11	Go trials		x	x	x				x									
Fassbender et al., 2006 ($p < .04$)	16	Cued CR			x				x	x	x								
Wager et al., 2005 ($p < .05$)	15	Go trials	x	x	x					x	x	x						x	
Kelly et al., 2004 ($p < .05$)	14	FA		x	x	x		x		x	x	x			x			x	x
Garavan et al., 2003 ($p < .01$)	16	FA		x	x			x			x								x
Mathalon et al., 2003 ($p < .05$)	10	Hits	x	x	x	x	x	x	x	x	x	x	x		x	x	x	x	x
Mostofsky et al., 2003 ($p < .05$)	48	Implicit		x															x
Garavan et al., 2002 *($p < .05$)*	14	Implicit			x	x		x		x	x								
Menon et al., 2001 ($p < .05$)	14	Go trials	x	x		x					x					x			
Liddle et al., 2001 *($p < .05$)*	16	Implicit & Go trials	x	x	x	x	x	x	x		x	x	x	x					x
Braver et al., 2001 ($p < .05$)	14	Go trials	x		x	x		x			x	x							
Kiehl et al., 2000 ($p < .001$)	14	Implicit	x		x								x		x				x
Garavan et al., 1999 ($p < .001$)	14	Go trials			x	x				x	x				x				